

# Stability and Confinement Properties of Auxiliary Heated NSTX Discharges

J.E. Menard<sup>1</sup>, R.E. Bell<sup>1</sup>, C. Bourdelle<sup>1</sup>, D.S. Darrow<sup>1</sup>, E.D. Fredrickson<sup>1</sup>, D.A. Gates<sup>1</sup>,  
L.R. Grisham<sup>1</sup>, S.M. Kaye<sup>1</sup>, B.P. LeBlanc<sup>1</sup>, R. Maingi<sup>2</sup>, S.S. Medley<sup>1</sup>, D. Mueller<sup>1</sup>,  
F. Paoletti<sup>3</sup>, S.A. Sabbagh<sup>3</sup>, D. Stutman<sup>4</sup>, D.W. Swain<sup>2</sup>, J.R. Wilson<sup>1</sup>, M.G. Bell<sup>1</sup>,  
J.M. Bialek<sup>3</sup>, C.E. Bush<sup>2</sup>, J.C. Hosea<sup>1</sup>, D.W. Johnson<sup>1</sup>, R. Kaita<sup>1</sup>, H.W. Kugel<sup>1</sup>,  
R.J. Maqueda<sup>5</sup>, M. Ono<sup>1</sup>, Y-K.M. Peng<sup>2</sup>, C.H. Skinner<sup>1</sup>, V.A. Soukhanovskii<sup>1</sup>,  
E.J. Synakowski<sup>1</sup>, G. Taylor<sup>1</sup>, G.A. Wurden<sup>5</sup>, S.J. Zweben<sup>1</sup>

<sup>1</sup> Princeton Plasma Physics Laboratory, Princeton, NJ 08543-0451, USA

<sup>2</sup> Oak Ridge National Laboratory, Oak Ridge, TN, USA

<sup>3</sup> Columbia University, New York, NY, USA

<sup>4</sup> Johns Hopkins University, Baltimore, MD, USA

<sup>5</sup> Los Alamos National Laboratory, Los Alamos, NM, USA

## 1. Introduction

The National Spherical Torus Experiment (NSTX) is a spherical tokamak with nominal plasma major radius  $R_0=0.85\text{m}$ , minor radius  $a=0.66\text{m}$ , and aspect ratio  $A > 1.28$ . Typical discharge parameters are  $I_p = 0.7\text{-}1.4\text{ MA}$ ,  $B_{t0} = 0.25\text{-}0.45\text{ Tesla}$  at  $R_0$ , elongation = 1.7-2.2, triangularity 0.3-0.5, line-average electron density  $n_e = 2\text{-}5 \times 10^{19}\text{ m}^{-3}$ ,  $T_e(0)=0.5\text{-}1.5\text{keV}$ , and  $T_i(0) = 0.5\text{-}2\text{keV}$ . The NSTX auxiliary heating systems can routinely deliver 4.5MW of 80keV deuterium neutral beams and 3MW of 30MHz high-harmonic fast wave power. Kinetic profile diagnostics presently include a 10 channel, 30Hz multi-pulse Thomson scattering system (MPTS), a 17 channel charge exchange recombination spectroscopy (CHERS) system, a 48 chord ultra-soft X-ray (USXR) array, and a 15 chord bolometry array. Initial experiments utilizing auxiliary heating on NSTX have focused on MHD stability limits, confinement trends, studying H-mode characteristics, and performing initial power balance calculations.

## 2. Experimental Results

### 2.1. MHD Stability

The spherical tokamak (ST) is expected to be stable to pressure-driven instabilities at high toroidal  $\beta = \beta_{t0} \equiv 2\mu_0\langle p \rangle / B_{t0}^2$ . Access to high  $\beta$  is achieved by operating at high normalized current  $= I_p / aB_{t0}$  and derives from the Troyon [1] relation for the no-wall  $\beta$ -limit in tokamaks,  $\beta_{\text{max}} \leq C_T I_p / aB_{t0}$  where  $C_T$  is a constant. Key issues for the ST include (a) the determination of the maximum achievable  $\beta_N \equiv \beta(\%)a(\text{m})B_{t0}(\text{T})/I_p(\text{MA})$  and (b) the definitions of  $\beta$  and  $\beta_N$  (if any) which allow the Troyon relation to accurately apply to all tokamak aspect ratios. EFIT [2, 3] analysis of nearly 900 NSTX discharges with  $I_p > 0.5\text{MA}$  has been performed using external magnetic measurements only. Good agreement is found between EFIT and the measured diamagnetic flux, and the sawtooth inversion radius as determined from USXR tomography is in good agreement with the  $q=1$  radius as found by EFIT.

The EFIT total stored energy tends to be 15-20kJ larger than the sum of thermal plus fast particle stored energy based on measured  $T_e$ ,  $n_e$ , and  $T_i$  profiles and assuming classical confinement and thermalization of NBI ions. This results in a 10-15% uncertainty in the highest NSTX  $\beta$  values. Figure 1 shows NSTX EFIT  $\beta$  values at peak stored energy plotted versus  $I_p/aB_{t0}$ . As seen in Figure 1a, NSTX has achieved  $\beta_N=2-4$  over a range of  $I_p/aB_{t0}$  spanning 2-6. Thus far, the highest  $\beta_N$  values have been achieved at the lowest toroidal field  $B_{t0} = 3\text{kG}$ , although recently NSTX has achieved  $\beta_{t0} = 20\%$  at  $I_p=1.2\text{MA}$  and  $B_{t0} = 3.5\text{kG}$ . Figure 1b, shows the same NSTX data using the definition of  $\beta$  originally used by Troyon [1]. As seen in the figure, using the volume average of  $B^2$  leads to  $\beta$  values roughly a factor of 2 lower than the conventional tokamak definition. With this definition of  $\beta$ ,  $\langle\beta_N\rangle \approx 2$  appears to better describe the  $\beta$ -limit of present NSTX discharges. Profile optimization will likely be required to reach the theoretical no-wall limit of  $\langle\beta_N\rangle \approx 3$ .

At the  $\beta$ -limit for the discharges of Figure 1, either rapid  $\beta$  collapse or  $\beta$  saturation is observed. The highest  $\beta$  shots in NSTX routinely suffer rapid collapses, and inspection of the data in Figure 1 reveals that these discharges typically have  $q(0)$  at or below 1 at collapse. For such discharges, ideal stability analysis shows that internal pressure-driven kink modes with toroidal mode numbers  $n=1-2$  (sometimes higher) can simultaneously become unstable. Figure 2a shows the frequency and toroidal mode number spectrum for a discharge with peak  $\beta=20\%$ . This discharge suffers a rapid  $\beta$  collapse at  $t=220\text{ms}$  and shows a large  $n=1$  (and smaller  $n=2$ ) mode active at the collapse. Prior to this collapse, several other mode numbers are present throughout the discharge. As seen in Figure 2a, a large 80kHz  $n=1$  mode appears shortly after beam turn-on. The mode frequency scales roughly with the Alfvén speed and is much higher than the initial plasma rotation frequency. Then, as  $q(0)$  approaches 1 near  $t=150\text{ms}$ , the  $n=1$

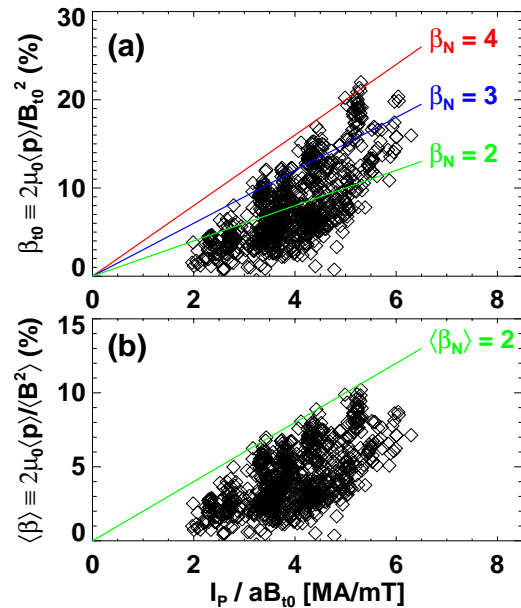


**Figure 1.** (a) Vacuum-toroidal beta and (b) volume-average beta versus  $I/aB$  for NSTX discharges with  $I_p > 500\text{kA}$ .

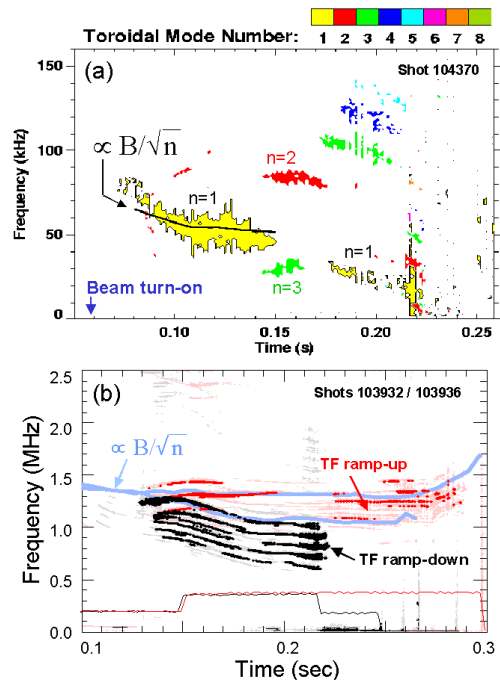


**Figure 2.** (a) Intermediate frequency (0-150kHz) MHD activity for a  $\beta=20\%$  discharge and (b) 0.2-2MHz MHD activity for lower  $\beta$  discharges undergoing TF ramps.

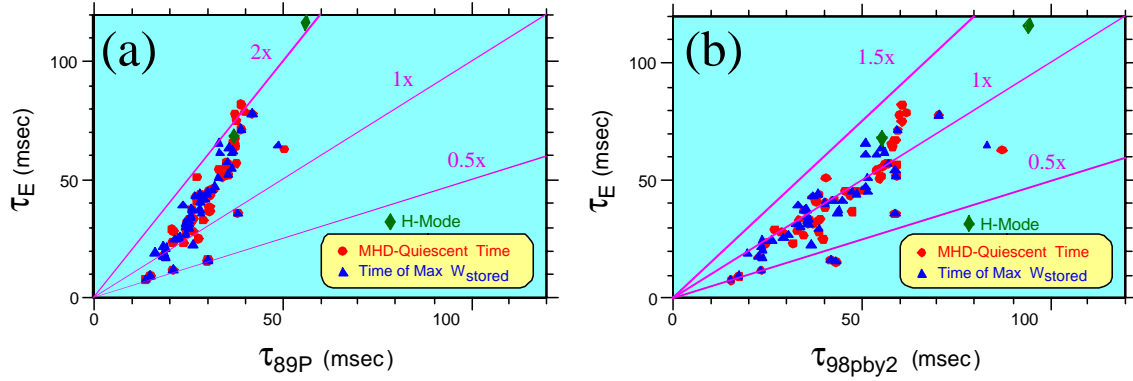


**Figure 3.** NSTX total energy confinement times compared to (a) ITER-89P and (b) 98pby2 scalings at peak stored energy (triangles) and MHD-quiescent time (circles).

mode disappears and  $n=2$  and  $3$  modes appear at completely different frequencies. If these modes are Toroidal Alfvén Eigenmodes (TAEs), continuum damping of the original  $n=1$  mode by the presence of the  $1/1$  surface may explain this phenomena. Later, as  $q(0)$  drops below  $1$ , the  $n=1$  (and higher) mode reappears and persists until the collapse. Not every NBI discharge has activity in this frequency range, and those that do have only minor fast ion losses when the modes are active. The highest  $\beta_p$  ( $\approx 0.4-0.5$ ) discharges in NSTX typically have higher  $q(0)$  and more frequently exhibit  $\beta$  saturation. Such discharges tend to have  $n > 1$  activity dominant during saturation. Neoclassical tearing modes are a very plausible cause of such saturation and are under active study.

Higher frequency NBI-driven MHD modes with  $f = 0.5-2\text{MHz}$  have also been observed in NSTX. Figure 2b shows the frequency spectra for two discharges - one with a toroidal field (TF) ramp-up, the second with a TF ramp-down. As seen in the figure, the mode frequency is observed to scale as the Alfvén speed which indicates that the modes are plasma eigenmodes rather than energetic particle modes [4]. These modes exhibit most of the properties of Compressional Alfvén Eigenmodes (CAE) [5] which can be excited through a Doppler-shifted perpendicular resonance with NBI fast ions at frequencies well below the ion cyclotron frequency where ion cyclotron and ion and electron Landau damping are weak. These modes cause no apparent fast ion loss, and in some circumstances are active when the lower-frequency TAE-like modes described above are also present.

## 2.2. Confinement

The achievement of high  $\beta$  in NSTX has been greatly facilitated by good energy confinement even in non H-mode discharges. Figure 3a compares the total (thermal+beam) energy confinement times of select NSTX discharges to the ITER-89P L-mode scaling. As seen in the figure, H-factors relative to 89P are in the range of  $1-2$  and increase as the confinement time increases. As expected, the highest confinement is achieved when MHD is not active (circles) or is weak. Figure 3b plots NSTX confinement against the 98pby2 H-mode scaling, and as seen in this figure, this scaling better matches NSTX for both H-mode and non H-mode discharges. Confinement times for two discharges with clear H-mode signatures are also plotted in the figure (green diamonds) and have  $H \approx 1.25$  relative to 98pby2. The spontaneous low-to-

high (L-H) confinement mode transitions have only been observed in lower-single-null divertor discharges for  $P_{\text{NBI}} > 850\text{kW}$  and  $B_{10}=0.45$  Tesla. The H-mode phase varies from 0.5-65ms in duration and is typically terminated by peripheral MHD in the form of cold  $m/n=2/1$  islands. The observation of clear H-mode transitions and profiles suggests that other high-confinement plasmas in NSTX are not transition-less H-modes. High-temperature bake-out of all NSTX graphite and control system upgrades are expected to further improve confinement in NSTX and hopefully allow easier access to H-mode.

Initial analysis of CHERS profiles obtained during NBI power step-ups shows that the  $T_i$  profiles can be broader and hotter than the  $T_e$  profiles. Figure 4a shows the ion (black) and electron (blue) temperatures for shot 104001 near  $t=290\text{ms}$ . This discharge has  $I_p=1\text{MA}$ ,  $B_{10}=4.5\text{kG}$ , and achieves  $\beta=9\%$  and a peak stored energy of 150kJ. Figure 4b shows that central rotation frequencies can approach 30kHz (200km/s) and outboard plasma edge rotation velocities are also quite high (40-50km/s). Flat spots in the angular rotation profile appear to be correlated with MHD activity near mode-rational surfaces, particularly near  $q=2$ . As seen in Figure 4a, the central ion temperature is  $\approx 2\text{keV}$  and significantly exceeds the electron temperature over most of the profile. The central electron density at  $t=297\text{ms}$  is  $4.3 \times 10^{19} \text{ m}^{-3}$  and is sufficiently high that strong electron-ion thermal coupling is expected. In fact, this coupling is computed (by TRANSP) to transfer 1.2MW from ions to electrons out of a total heating power of 1.75MW (1.5MW NBI). This results in a negative computed ion thermal conduction. Possible explanations of this situation include missing neoclassical corrections to the ion-electron coupling and anomalous ion heating [6]. Future experiments will attempt to better understand which plasma regimes exhibit this unusual behavior.

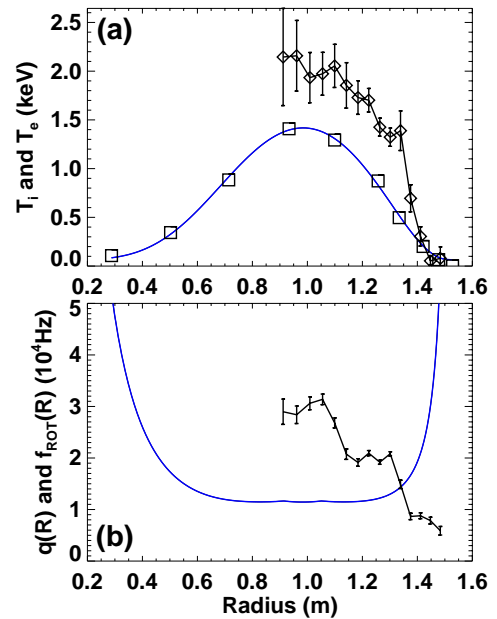


**Figure 4.** (a) Electron (blue) and ion temperature profiles and (b) safety factor (blue) and carbon rotation frequency profiles ( $\div 10\text{kHz}$ ) for shot 104001 near  $t=290\text{ms}$ .

## Acknowledgments

This work was supported by the United States Department of Energy under contract numbers DE-AC02-76CH03037 (PPPL), DE-AC05-00R22725 (ORNL), W-7405-ENG-36 (LANL) and grant numbers DE-FG02-99ER54524 (CU), DE-FG02-99ER54523 (JHU).

## References

- [1] F. Troyon *et al.*, Plasma Phys. and Contr. Fus. **26**, 209 (1984).
- [2] L. L. Lao *et al.*, Nucl. Fus. **25**, 1611 (1985).
- [3] S. A. Sabbagh *et al.*, Nucl. Fus. (2001), accepted for publication.
- [4] E. D. Fredrickson *et al.*, to be submitted to Phys. Rev. Lett.
- [5] N. Gorelenkov and C. Cheng, Nucl. Fus. **35**, 1743 (1995).
- [6] D. A. Gates, R. White, and N. Gorelenkov, submitted to Phys. Rev. Lett.